

# Calorimetric glass transition in a mean-field theory approach

Manuel Sebastian Mariani<sup>a</sup>, Giorgio Parisi<sup>b,c,1</sup>, and Corrado Rainone<sup>b,d,1</sup>

<sup>a</sup>Department of Physics, University of Fribourg, CH-1700 Fribourg, Switzerland; <sup>b</sup>Dipartimento di Fisica, Sapienza Università di Roma, I-00185 Rome, Italy;  
<sup>c</sup>Istituto Nazionale di Fisica Nucleare, Sezione di Roma I, Istituto per i Processi Chimico-Fisici, Consiglio Nazionale delle Ricerche, I-00185 Rome, Italy;  
and <sup>d</sup>Laboratoire de Physique Théorique, École Normale Supérieure, UMR 8549 CNRS, 75005 Paris, France

The study of the properties of glass-forming liquids is difficult for many reasons. Analytic solutions of mean-field models are usually available only for systems embedded in a space with an unphysically high number of spatial dimensions; on the experimental and numerical side, the study of the properties of metastable glassy states requires thermalizing the system in the supercooled liquid phase, where the thermalization time may be extremely large. We consider here a hard-sphere mean-field model that is solvable in any number of spatial dimensions; moreover, we easily obtain thermalized configurations even in the glass phase. We study the 3D version of this model and we perform Monte Carlo simulations that mimic heating and cooling experiments performed on ultrastable glasses. The numerical findings are in good agreement with the analytical results and qualitatively capture the features of ultrastable glasses observed in experiments.

glass transition | mean-field theory | ultrastable glasses | planting | replica theory

The theoretical interpretation of the properties of glasses is highly debated. There are two extreme viewpoints:

- One approach, the random first-order transition (RFOT) theory (1), which uses mostly the replica method (2) as its central tool, assumes that the dynamical properties of glasses do reflect the properties of the appropriate static quantities [such as the Franz–Parisi potential (3); for a review see refs. 2 and 4].
- The other approach, kinetically constrained models (KCMs), assumes that the glass transition is a purely dynamical phenomenon without any counterpart in static quantities (5–7).

The mean-field version of the RFOT approach predicts the presence of a dynamical transition [identified with the mode-coupling transition (8)] at a nonzero temperature  $T_d$ , whereupon the configuration space of the glass former splits into a collection of metastable states. Below  $T_d$  the system will remain trapped inside a metastable state. Beyond mean-field theory the dynamical transition  $T_d$  becomes a cross-over point: At  $T_d$  the correlation time and the dynamical correlation length become very large, but finite. Below  $T_d$ , the relaxation time increases rapidly and becomes comparable with human timescales, leading to the phenomenological glass transition. In the KCM approach this slowdown is a phenomenon originated only by constraints on the dynamics, whereas the RFOT picture views the off-equilibrium states as metastable, thermodynamic states, that can be identified with the minima of a suitable equilibrium free-energy functional and then studied using a modified equilibrium formalism, generally built on the replica method.

According to replica formalism, the system explores the whole collection of possible states, with lower and lower free energy, as the temperature is lowered from  $T_d$  to another temperature  $T_K$  (the Kauzmann temperature), where the states with the lowest free energy are reached. Most RFOT models (but actually not all, because  $T_K=0$  for some models) predict then an equilibrium phase transition at  $T_K$ , with a real divergence of the relaxation time.

To test this scenario, it would be necessary to perform experiments and simulations at various temperatures in this range, but then one must face the problem of equilibrating the glass former at temperatures  $T \approx T_K \ll T_g$  (where  $T_g$  is the phenomenological glass transition temperature), where it is by definition impossible to do so. Indeed, a simple estimate shows that the increase of the equilibration time below  $T_d$  is so sharp that one cannot get nearer to  $T_K$  than  $\Delta T \approx \frac{1}{3}T_K$  without falling out of equilibrium, making it impossible for us to get a good look at the lowest states: Only the high free-energy states near  $T_d$  can be probed experimentally.

Some progress in this direction has been made recently both in experiments (9) and numerical simulations (10), with the introduction of the so-called vapor deposition technique, which allows one to obtain extraordinarily stable glasses [usually referred to as ultrastable glasses (10–13)] in a relatively short time, even for temperatures much lower than  $T_d$ . First numerical simulations on an ultrastable glass of binary Lennard-Jones mixture seem to support the existence of a thermodynamic phase transition (10). On the theoretical side, the intrinsic out-of-equilibrium nature of glass poses another challenge, because the methods of equilibrium statistical mechanics cannot be used in the usual way, requiring, in principle, to resort to dynamical tools. This strategy is actually viable and was used, for example, by Keys et al. (14), where a suitably tuned East model has been shown to reproduce well the experimental behavior observed in DSC (differential scanning calorimetry) experiments on different glass-former materials, for example glycerol (15) and boron oxide (16). This approach, however, has the drawback of being phenomenological in nature.

The recent introduction (17) of a semirealistic soluble model for glasses, the Mari–Kurchan (MK) model, gives us the possibility of addressing both the equilibration and the theoretical problem. It allows us to obtain equilibrated configurations also

## Significance

Understanding the properties of glasses is one of the major open challenges of theoretical physics. Making analytical predictions is usually very difficult for the known glassy models. Moreover, in experiments and numerical simulations thermalization of glasses cannot be achieved without sophisticated procedures, such as the vapor deposition technique. In this work we study a glassy model that is simple enough to be analytically solved and that can be thermalized in the glassy phase with a simple numerical method, opening the door to an intensive comparison between replica theory predictions and numerical outcomes.

Author contributions: G.P. designed research; M.S.M., G.P., and C.R. performed research; and M.S.M., G.P., and C.R. wrote the paper.

The authors declare no conflict of interest.

<sup>1</sup>To whom correspondence may be addressed. Email: giorgio.parisi@roma1.infn.it or Corrado.Rainone@roma1.infn.it

This article contains supporting information

beyond the dynamical transition and deep into the glass phase, using the so-called planting method (18). Moreover, it is in principle solvable in the replica method, allowing us to study the metastable glassy states with a static formalism, without having to solve the dynamics.

Our aim is to use this model to simulate slow annealing experiments usually performed on glasses and ultrastable glasses, to compare the numerical outcomes with experimental results and theoretical predictions in the replica method.

### The Model

We consider the potential energy of the family of models introduced by Mari and Kurchan (MK model) (17):

$$V(\underline{x}, \underline{l}) = \sum_{(i,j)} v(\mathbf{x}_i - \mathbf{x}_j - \mathbf{l}_{ij}), \quad [1]$$

where  $\underline{x} = \{\mathbf{x}_1, \dots, \mathbf{x}_N\}$  are  $N$   $d$ -dimensional vectors, representing particles positions, and the particles move in a  $d$  dimensional cube of size  $L$ , with periodic boundary conditions. The main feature of the model are the variables  $\underline{l} = \{\mathbf{l}_{ij}\}$ : They are  $N(N-1)/2$  quenched random vectors, called random shifts, independently drawn out from a uniform probability distribution inside the cube. The function  $v$  could be in principle any interesting short-ranged repulsive pairwise interaction.

The main effect of the random shifts is to destroy the direct correlation among the particles that interact with a given particle (17). This makes the computation of static quantities very simple, because in the Mayer expansion of the grand-canonical potential only the tree diagrams survive in the thermodynamic limit (17). The idea is quite old (19), and had important applications to turbulence, but has only recently been applied to glasses.

**Static Thermodynamic Properties in Liquid Phase.** Here we will summarize analytical and numerical results obtained by Mari and Kurchan for this model. In the following  $D$  will denote the diameter of spheres. In hard-sphere systems the potential  $v(\mathbf{x})$  is infinite at distances less than  $D$  and the role of inverse temperature is played by the packing fraction  $\varphi = N\mathcal{V}_d(D)/L^d = \rho\mathcal{V}_d(D)$ , where  $\mathcal{V}_d(D)$  is the volume of the  $d$ -dimensional sphere of diameter  $D$ ; we will call it density absorbing the multiplicative factor in its definition.

The Hamiltonian contains random terms and the interesting quantities have then to be averaged over these parameters. We can define the annealed entropy  $S^A$  and the quenched entropy  $S^Q$  given by

$$S^A \equiv \log(\overline{Z(\underline{l})}), \quad S^Q \equiv \overline{\log(Z(\underline{l}))}. \quad [2]$$

The computation of  $S^A$  can be easily done and one finds

$$S^A(\rho) = \frac{S^A(\rho)}{N} = -\log(\rho) - 2^{d-1} \mathcal{V}_d(D) \rho + \log(N). \quad [3]$$

The presence of the  $\log(N)$  term is due to the fact that in this model particles are distinguishable for a given realization of random shifts.

A more interesting quantity is the quenched entropy. In this model one finds that  $S^A(\rho) = S^Q(\rho)$  in the liquid phase (i.e., below the Kauzmann transition density  $\varphi_K$ ). The Kauzmann transition is avoided in the thermodynamic limit: The total entropy  $s^A$  grows as  $\log(N)$  whereas the vibrational entropy is a non-decreasing function of  $\rho$  that diverges in the infinite-density limit. This implies that the configurational entropy contains a term proportional to  $\log(N)$ . As a consequence, the Kauzmann density  $\varphi_K$  (i.e., the point where the configurational entropy vanishes) diverges logarithmically in the thermodynamic limit.

Using standard thermodynamic relations one can derive from Eq. 3 the liquid-phase equilibrium equation of state

$$P = \rho + 2^{d-1} \mathcal{V}_d(D) \rho^2, \quad [4]$$

where  $P$  is the pressure.

For what concerns the radial distribution function, one has to take the random shifts into account:

$$g(r) = \frac{1}{\rho^2} \left\langle \overline{\sum_{i \neq j}^N \delta(|\mathbf{x}_i - \mathbf{x}_j + \mathbf{l}_{ij}| - r)} \right\rangle, \quad [5]$$

where the bracket average is computed using the ensemble distribution function (Gibbs–Boltzmann distribution at equilibrium) and the bar average is computed using the random shifts probability distribution. The result is

$$g(r) = \theta(r - D), \quad [6]$$

where  $\theta$  is the usual Heaviside step function. This result is the same obtained with high-dimensional hard spheres (20), but the mean-field nature of the model has allowed us to get it in any number of spatial dimensions. The equilibrium pressure is related to density by the usual relation for hard spheres (21),

$$P = \rho + 2^{d-1} \mathcal{V}_d(D) g(D) \rho^2, \quad [7]$$

from which, using Eq. 6, the equilibrium equation of state (Eq. 4) can be derived again.

**Glassy Properties.** The model is interesting because despite the extreme simplicity of the statics (a feature that it has in common with facilitated models) the dynamics is extremely complex. At high densities there is the glass phase that in the thermodynamic limit is separated from the liquid phase by a mode coupling transition. This transition exists only if we embed the model in a space with an infinite number of dimensions  $d$ ; when  $d < \infty$ , hopping effects destroy the transition, which becomes only a cross-over region (22).

Accurate simulations (22) give a higher value for the mode-coupling dynamical density (i.e.,  $\varphi_d = 1.91$ ). A more careful analysis of the properties of the system near the putative mode-coupling transition can be found in ref. 22, where the effects of hopping are carefully studied. Other features, such as a violation of the Stokes–Einstein relation and dynamical heterogeneities, are present in this model (17, 22).

### Numerical Simulations

When a glass is gradually heated during DSC experiments thermodynamic quantities, like the internal energy, continue to follow the glassy behavior also in the liquid phase, until the so-called onset temperature  $T_{on}$  is reached. For  $T > T_{on}$  the system gradually approaches equilibrium; during this relaxation process the specific heat reaches a maximum value, higher than the equilibrium one. The value of  $T_{on}$  quantifies the stability of the initial glass and is considerably higher for glasses prepared through the vapor deposition technique than ordinary glasses aged for many months (9, 10). The vapor deposition procedure has been recently mimicked by a computer algorithm, and numerical simulations over a Lennard-Jones binary mixture showed the same behavior (10, 11).

We aim to study numerically this deviation from equilibrium in the liquid region and the subsequent relaxation process in the MK model. In the MK model we are able to obtain equilibrium configurations beyond the dynamic transition via a special procedure, allowed only by the presence of random shifts, the

so-called planting (18) method. Basically, planting consists of two steps: the generation of a random configuration of sphere positions, independently drawn out from the uniform distribution over the volume, and the generation of the random shifts configuration  $\{\mathbf{l}_{ij}\}$  so that the nonoverlap condition imposed by the hard-sphere potential energy (Eq. 1) is satisfied for every pair of spheres (see *Supporting Information* for details). The mean-field nature of the interaction guarantees that planted configurations are equilibrated (18). The planted glass in the MK model, like vapor-deposited ultrastable glasses in real world, is the best possible starting point for the study of the deviation from equilibrium in the liquid phase. We start from a planted configuration and mimic DSC heating experiments by running adiabatic stepwise decompression scans, where the system performs jumps between different density values and a large number of Monte Carlo steps for each density value, to reach thermalization.

We refer to *Supporting Information* for all other simulation details. We present now the results of numerical simulations, based on the Monte Carlo method, of a system composed of  $N=800$  spheres of diameter  $D=1$  in  $d=3$  dimensions, with periodic boundary conditions.

**Decompression Jump and Spheres Contact Region Emptying.** The outcome of the planting technique is a thermalized initial configuration at a certain density  $\varphi_0 > \varphi_d$  (see Fig. S1). We discuss now the effects a density jump  $\varphi_0 \rightarrow \varphi_1$  on  $g(r)$ , where  $\varphi_1 < \varphi_0$  (decompression). Results for  $\varphi_0=2.5$  and  $\varphi_1=1.7$  are shown in Fig. 1. When the sphere radius is decreased, particles originally in contact separate, causing a drop of  $g(r)$  in the contact region  $r \sim 1$ . While the system evolves at the new density value  $\varphi_1$ , gradually particles return in contact, causing the filling of the contact zone. In the glass phase this filling can only be partial for realizable time scales. In the liquid region and for densities sufficiently far from the dynamical transition it is possible to see a complete filling.

We consider now the following decompression protocol: We start from a planted configuration at  $\varphi_0=2.5$ , we jump to  $\varphi_1=1.6$  and wait  $2^{22}$  steps, then we jump to  $\varphi_2=1.55$  and we wait again  $2^{22}$  steps, then  $\varphi_3=1.5$  and  $\varphi_4=1.45$ . Fig. 2 shows the temporal behavior of  $g(1)$  for various values of  $\varphi$ . We do not see structural relaxation for  $\varphi=1.55, 1.5$  (liquid phase): the system, after a partial, fast relaxation process reaches the metastable

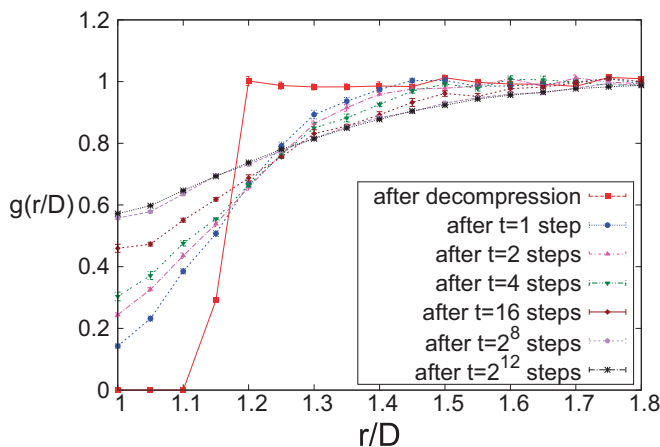


**Fig. 1.** Radial distribution function  $g(r)$  for  $\varphi_1 = 1.7$  at various times  $t$ , starting from a thermalized initial configuration at  $\varphi_0 = 2.5$ . Immediately after the density jump, there are no particles in contact and  $g(r)$  shows a drop where  $r \sim D$  (red points). While the system evolves at the new density value  $\varphi_1 = 1.7$ , spheres gradually return in contact, partially filling the dip.

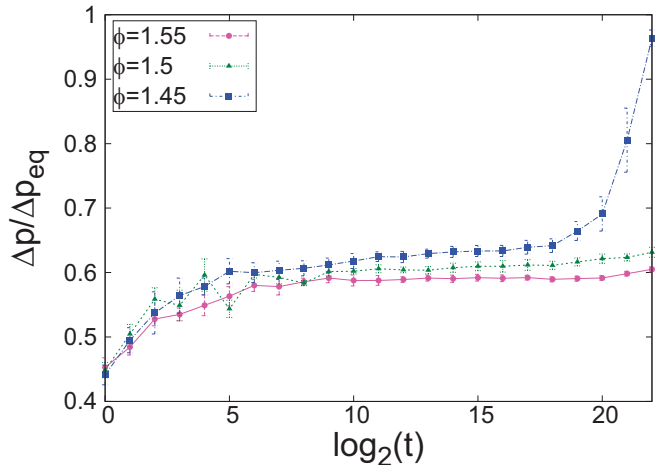


**Fig. 2.** Temporal behavior of the ratio  $\Delta p / \Delta p_{eq} = g(1)$  between the excess pressure  $\Delta p = p - 1$  and the equilibrium value  $\Delta p_{eq}$  for various  $\varphi$  values in the liquid phase, for the decompression protocol with  $\varphi_0 = 2.5$ ,  $\varphi_1 = 1.6$ ,  $\varphi_2 = 1.55$ ,  $\varphi_3 = 1.5$ ,  $\varphi_4 = 1.45$ . We do not show the curves for  $\varphi = \varphi_0 = 2.5$  (planted configuration,  $g(1) = 1$ ) and  $\varphi = \varphi_1 = 1.6$ , not comparable with  $\varphi = 1.55, 1.5, 1.45$  because the system reaches  $\varphi = 1.6$  after a larger density jump. Only for  $\varphi = 1.45$  we can observe a clear sign of structural relaxation, whereas for higher densities the system remains trapped in the original metastable state.

plateau and it does not have enough time to escape. When  $\varphi = 1.45$ , the lifetime of the original metastable state is smaller than  $2^{22}$  steps and we observe a clear structural relaxation, corresponding to the complete filling of the contact zone.

**Mean Square Displacement and Structural Relaxation Time.** To study the behavior of the relaxation time as a function of density in the liquid phase and evaluate the dynamic glass transition density  $\varphi_d$ , we turn our attention to another observable, the mean square displacement  $\Delta(t)$  (MSD) of spheres from their initial positions:

$$\Delta(t) = \frac{1}{N} \sum_{i=1}^N |\mathbf{x}_i(t) - \mathbf{x}_i(0)|^2. \quad [8]$$

Because we are interested only in the relaxation time, we start from a thermalized configuration at  $\varphi_0 = 2.5$  and we jump directly to the density value  $\varphi$  we are studying. We stress that in Eq. 8  $\mathbf{x}_i(0)$  is physical position of sphere  $i$  immediately after the density jump. We let the system evolve for  $2^k$  steps at this density  $\varphi$ . For  $\varphi < \varphi_d$ , as expected in a glassy system not too far from its dynamical glass transition, we can observe a two-step relaxation process: The system reaches a metastable plateau after about  $2^{10} - 2^{11}$  steps, remains trapped in it for a long time, after which structural relaxation occurs. For each value of density we fitted the MSD's escape from the plateau with a power law function and obtained the value of the relaxation time (see *Supporting Information* for details). We fitted the resulting curve of  $\tau_R$  as a function of  $\varphi$ , displayed in Fig. 3, with the power law behavior  $\tau_R = A(\varphi_0 - \varphi)^{-\gamma}$ , obtaining in this way  $\varphi_0 = 1.73 \pm 0.04$ ,  $\gamma = 4.1 \pm 0.7$ . One can notice that the value for  $\gamma$  is not too different from the one obtained in ref. 17 performing a similar analysis on the relaxation time, whereas the value of  $\varphi_0$  is definitely smaller than  $\varphi_d$ , but not too far from the one obtained in ref. 17.

**Decompression and Compression Scans: Qualitative Comparison with Experiments.** In Fig. 4 we represent the behavior of the reduced pressure  $p = P/\rho$  as a function of density for a decompression protocol with starting density  $\varphi_0 = 2.5$  and a constant density-jump amplitude  $\Delta\varphi = \varphi_n - \varphi_{n-1} = \varphi_1 - \varphi_0$ . We have different curves for

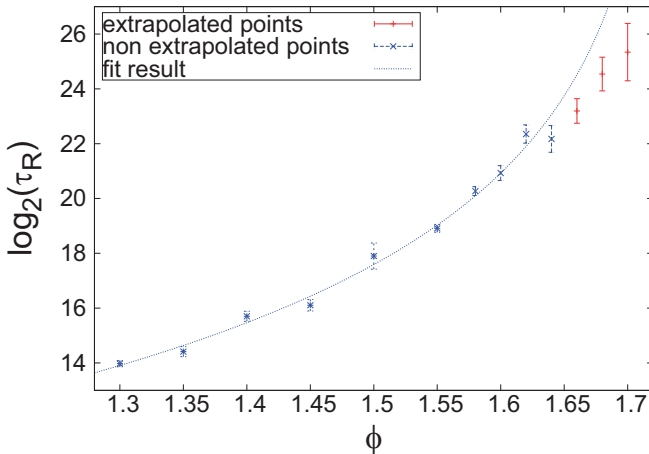


**Fig. 3.** Relaxation time as a function of density, computed as described in the text. Red points are the result of an extrapolation (when  $\tau_R$  is larger than the largest number of performed Monte Carlo steps at each density value, i.e.,  $2^{22}$  steps) so they were discarded in the fit. Blue line is the fit result.

different values of the number  $2^k$  of Monte Carlo steps performed at each density value. For sufficiently high  $\varphi$ , we see a deviation from equilibrium independent from the decompression rate. For values well above  $\varphi_d$ , for example  $\varphi=2.0$ , the system is in the glass phase, so relaxation takes place inside the original metastable state and pressure deviates from its equilibrium value. This deviation continues for the largest density values below  $\varphi_d$ , for example  $\varphi=1.6, 1.65, 1.7$ : The system continues to relax inside the original metastable state, not yet having sufficient time to reach equilibrium. When density is sufficiently low, the lifetime of the original metastable state becomes smaller than  $2^k$  and the onset of relaxation toward equilibrium takes place. The relatively sharp pressure reclimb is dependent on decompression rate, and it is faster for slower rates.

The decompression protocol adopted for our system, composed by hard spheres, is equivalent to the typical DSC's heating scans, with two crucial differences. (i) In DSC experiments we move toward the glassy phase by decreasing the temperature: In the case of hard spheres the inverse of the density plays the same role of the temperature. (ii) The starting configurations of the dynamics are fully equilibrated and this corresponds only to the case of DSC with infinitely slow cooling speed and relatively fast heating speed. The observed deviation of pressure from equilibrium for  $\varphi < \varphi_d$  is qualitatively the same phenomenon typically observed in DSC experiments. One point is important to note: In DSC experimental heating data the relaxation toward equilibrium for  $T > T_{on}$  is gradual and smooth (9), internal energy and enthalpy are continuous at the onset point and the specific heat gradually reaches its maximum value, whereas in Fig. 4 the reclimbing of pressure seems relatively sharp, probably signaling an underlying singularity (with infinite compressibility).

In Fig. 5 curves for different values of  $\varphi_0$  are represented, corresponding to different metastable states. The performed scans start from a planted configuration, corresponding to a point on the equilibrium line, and lead the system to a pressure lower than the equilibrium value during decompression. As expected, during decompression the relaxation of pressure toward equilibrium is sharp and starts at a lower onset density the higher  $\varphi_0$  is, that is, the more stable is the original glassy configuration: The system has memory of the initial state of the glass (hysteresis). This effect is analogous to what is observed in ultrastable real glasses (9): The more stable the initial glass obtained via vapor deposition is, the longer is the deviation from equilibrium in the liquid phase and, as a result, the higher is the onset temperature. When we compress the system

(only from  $\varphi_0=2.5$  in Fig. 5), pressure becomes higher than the equilibrium one, as expected. This effect mirrors what happens in decompression and the two sets of data concerning decompression and compression scans from  $\varphi_0=2.5$  join smoothly, as expected.

### Replica Computation of Metastable States Curves

So far we have shown how the MK model allows one to prepare the system in a glass state, even at densities much higher than the dynamical one, without incurring the problem of extremely large equilibration times. In addition, this model has another remarkable advantage: It is in principle solvable, thanks to its mean-field nature. The interaction network is tree-like (or, alternatively, without loops) in the thermodynamic limit, like in Van der Waals liquids (17, 21), and thus it also allows for a ready comparison between numerics and analytic computations. In particular, it allows us to perform computations in the replica method. Although the MK model is soluble, its actual analytic solution is exceedingly complex (23), so we have to resort to some kind of approximation: Here we assume that the cages have a Gaussian shape (22).

In the replica approach to the glass transition (1, 4), it is assumed that for densities  $\varphi > \varphi_d$  the configuration space can be unambiguously split in subsets, denoted as metastable glassy states. These states are theoretically identified with the local minima of a suitable functional, which plays in this context the same role of the Thouless–Anderson–Palmer free energy in spin glasses (2). In a mean-field situation and in the thermodynamic limit, where metastable states live forever, the system becomes then immediately trapped in one of these states and fails permanently to attain relaxation (the so-called mode coupling transition). However, out of mean field or with finite system size the system will be finally able to hop out of the state (22) and relax, although an extremely long time will be needed to do so (5).

The most important feature of these metastable states is that they are degenerate, that is, they can have the same free entropy. In fact, if one fixes a density  $\varphi > \varphi_d$  and a value  $s$  for the free entropy, it is possible to see that the number of states that share it (in the functional picture, the number of minima that all have the same height  $s$ ) scales exponentially with the size of the system,  $\mathcal{N}(s, \varphi) \propto e^{\Sigma(s, \varphi)N}$ . This causes the total free entropy of the system to gain an extra term to take this fact into account:

$$S(s, \varphi) = s + \Sigma(s, \varphi),$$

where  $\Sigma(s, \varphi)$  is called complexity (or, alternatively, configurational entropy), a central quantity in replica theory.

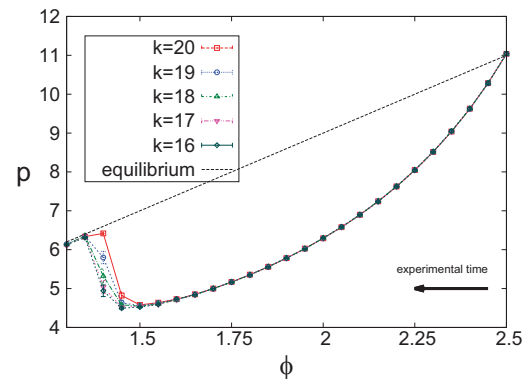


**Fig. 4.** Reduced pressure  $p$  as a function of density in a decompression protocol with  $\varphi_0=2.5$ ,  $\Delta\varphi=-0.05$ . Different colors correspond to different decompression rates ( $k$  is the number of Monte Carlo steps performed at each density value).

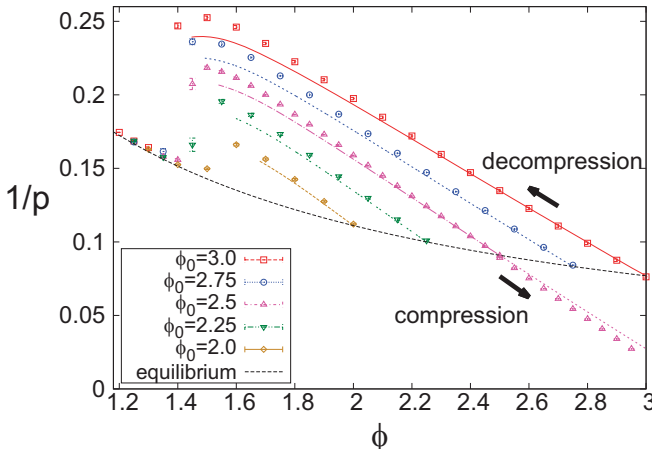


**Fig. 5.** Inverse of the reduced pressure  $p$  as a function of density during compression and decompression scans. Different colors correspond to different values of the planting density  $\phi_0$ . Points are the results of the Monte Carlo numerical simulations and lines are the analytical results obtained from the replica method within the isocomplexity assumption, as described in the text. The black line represents the equilibrium pressure (Eq. 4). and black arrows indicate the direction of experimental time, which runs from right to left during decompression scans (points above the equilibrium line) and from left to right during compression (points below the equilibrium line).

**The Replica Method.** The replica method provides us with a standard procedure to compute the complexity and also the in-state entropy (24). Its concrete application to hard-sphere systems is described in full detail in section III of ref. 4; here we recall it briefly. It consists of introducing  $m$  independent replicas of the system and forcing them to occupy the same metastable state. The entropy of the replicated system becomes then

$$S(m, \varphi) = \Sigma(\varphi, s) + ms(\varphi),$$

where  $s$  is the free entropy of the state. In the thermodynamic limit, the partition function will be dominated with probability 1 only by the states with the entropy  $s_{eq}$  that satisfies the optimum condition

$$\frac{d\Sigma(s, \varphi)}{ds} + m = 0. \quad [9]$$

The in-state entropy  $s_{eq}(m, \varphi)$  of those states and their complexity  $\Sigma_{eq}(m, \varphi)$  can then be derived using the following relations:

$$s_{eq}(m, \varphi) = \frac{\partial S(m, \varphi)}{\partial m}, \quad [10]$$

$$\Sigma_{eq}(m, \varphi) = m^2 \frac{\partial [m^{-1} S(m, \varphi)]}{\partial m}, \quad [11]$$

and the function  $\Sigma(s, \varphi)$  can then be reconstructed from the parametric plots of  $s_{eq}(m, \varphi)$  and  $\Sigma(m, \varphi)$ .

**Isocomplexity Approximation.** The replica formalism has been applied to the study of infinite dimensional hard spheres in a series of papers (20, 25, 26) with remarkable success. However, those results concern only the properties of the glass former after equilibration, whereas our numerical results concern the glass former when it is still trapped inside a metastable state, before equilibration takes place. Indeed, one could argue that, for experimental and practical purposes, getting predictions for this regime is even more important than the study of the equilibrium solution for infinite waiting times. This program, however, poses a challenge because in principle it requires solving the dynamics

for different preparation protocols. To this day, the only first-principles dynamical theory for glass formers is the mode coupling theory (8), which performs well near the dynamical transition but notoriously fails at higher densities, forcing one to use phenomenological models for the description of the high-density (or low-temperature) regime, as done by Keys et al. (14). We present here a computation that has the advantage of being both fairly simple and static in nature.

Because the system is trapped in a single metastable state during the simulation, it is clear that its physical properties are determined only by the in-state entropy  $s(\varphi)$  of that single state. We can easily determine  $s_{eq}$  at the beginning of the experiment, when the system is at equilibrium and it corresponds to  $s_{eq}(\varphi_0, 1)$ , but it is nontrivial to determine it when the density is changed and the system falls out of equilibrium, because Eq. 9 allows us to compute only quantities related to the states that dominate the partition function. Indeed, we can see that for every density  $\varphi$  we can choose the value of  $s_{eq}$  simply by appropriately tuning the parameter  $m$ , but in principle we still have no way of knowing what is actually the state the system is trapped into, that is, we lack a criterion to choose a function  $m(\varphi)$  consistent with the requirement that the system remain trapped in a single metastable state (27).

To overcome this difficulty, we assume that every state can be followed in density without any crossings between states, or bifurcations, or spinodal points (28); this means that the number (and thus the complexity) of states that share the same value  $s$  of the in-state entropy is a conserved quantity during the experiment and can then be used as a label for the states. This method is usually referred to as isocomplexity (27, 28).

In summary, to choose  $m(\varphi)$  we impose that

$$\Sigma(m(\varphi), \varphi) = \Sigma(1, \varphi_0) = \Sigma_0 = const. \quad [12]$$

This assumption is false in most cases. For example, it has been recently shown that for infinite-dimensional hard spheres a full replica symmetry breaking scenario holds for sufficiently high density (26), invalidating the isocomplexity hypothesis. The only exact method to tackle the problem would then be the state-following approach, which uses the two-replica potential as a central tool (3). However, this method is far more complex and its application goes beyond the scope of this paper; here we always use the isocomplexity approximation, referring to ref. 29 for the complete state-following computation. For a systematic comparison of the different approaches in the context of p-spin glasses, see ref. 30.

We refer to *Supporting Information* for the details of the computation of the isocomplexity lines displayed in Fig. 6. Once the potential  $s_{eq}^\Sigma(\varphi) = s_{eq}(m_\Sigma(\varphi), \varphi)$  has been obtained, one can compute

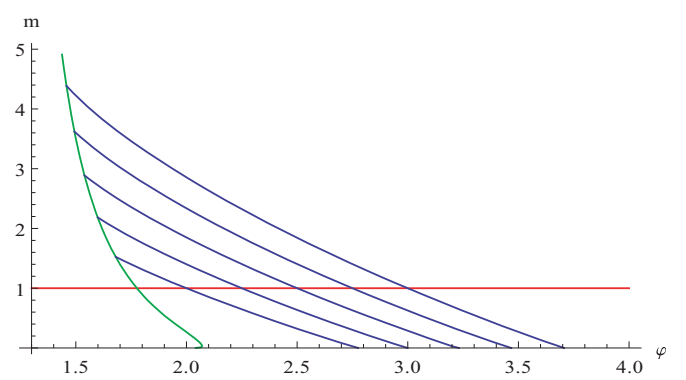


**Fig. 6.** Isocomplexity curves (blue lines) in the  $(m, \varphi)$  plane for  $\varphi_0 = 2.25, 2.5, 2.75, 3$ . Green line is the clustering line.

the desired physical observables using standard thermodynamic relations (21). Final results for pressure during decompression and compression are shown in Fig. 5 and compared with simulation results. There is a good agreement between analytical and numerical curves, especially for density values not too far from  $\varphi_0$ .

## Conclusions

We studied a mean-field model of glass transition, the MK model. We were able both to obtain a stable glass, thanks to the planting technique, and to study numerically and analytically (within replica method and isocomplexity assumption) the variations of pressure caused by relatively fast changes of density. We showed, both numerically and analytically, that qualitatively this model displays the same behavior of experimental ultrastable glasses reported in refs. 9 and 10. Our model seems to show a first-order phase transition when evading from metastable equilibrium (see ref. 29 and *Supporting Information*). This is in qualitative agreement with experiments, which show that the melting of ultrastable glasses (12, 13) has some features in common with first-order transitions.

We have also shown that the RFOT approach, together with the replica method, is able to qualitatively describe the process of glass formation through a slow annealing, with very little computational cost and without resorting to a posteriori phenomenological considerations. Our results can be compared with the DSC experiments where cooling is much slower than heating and as a result the cooled configurations (before heating) may be approximated with equilibrium configurations. We can study this situation in the MK model just because we can plant a thermalized equilibrium configuration at the density we prefer. The very interesting problem of understanding the behavior of DSC experiments when the cooling speed is the same (or faster) than the heating speed is not studied in this paper: In this situation analytic computations could be done only if we had the dynamics under analytic control, a goal that has not yet been reached.

**ACKNOWLEDGMENTS.** We thank Francesco Zamponi for useful discussions. This work was supported by the European Research Council (ERC) under the European Union's Seventh Framework Programme (FP7/2007-2013), ERC Grant 247328.

1. Kirkpatrick TR, Thirumalai D, Wolynes PG (1989) Scaling concepts for the dynamics of viscous liquids near an ideal glassy state. *Phys Rev A* 40(2):1045–1054.
2. Mezard M, Parisi G, Virasoro MA (1986) *Spin Glass Theory and Beyond*. World Scientific Lecture Notes in Physics (World Scientific, Singapore), Vol 9.
3. Franz S, Parisi G (1995) Recipes for metastable states in spin glasses. *J Phys I France* 5(11):1401–1415.
4. Parisi G, Zamponi F (2010) Mean field theory of hard sphere glasses and jamming. *Rev Mod Phys* 82(1):789.
5. Cavagna A (2009) Supercooled liquids for pedestrians. *Phys Rep* 476(4-6):51–124.
6. Ritort F, Sollich P (2003) Glassy dynamics of kinetically constrained models. *Adv Phys* 52(4):219–342.
7. Garrahan JP, Chandler D (2002) Geometrical explanation and scaling of dynamical heterogeneities in glass forming systems. *Phys Rev Lett* 89(3):035704.
8. Goetze W (2009) *Complex Dynamics of Glass-Forming Liquids: A Mode-Coupling Theory* (Oxford Univ Press, Oxford).
9. Swallen SF, et al. (2007) Organic glasses with exceptional thermodynamic and kinetic stability. *Science* 315(5810):353–356.
10. Singh S, Ediger MS, de Pablo JJ (2013) Ultrastable glasses from *in silico* vapour deposition. *Nat Materials* 12(2):139–144, and correction (2014) 13(6):662.
11. Parisi G, Sciotino F (2013) Structural glasses: Flying to the bottom. *Nat Mater* 12(2):94–95.
12. Lyubimov I, Ediger MD, de Pablo JJ (2013) Model vapor-deposited glasses: Growth front and composition effects. *J Chem Phys* 139(14):144505.
13. Sepúlveda A, Tyliński M, Giuseppi-Elie A, Richert R, Ediger MD (2014) Role of fragility in the formation of highly stable organic glasses. *Phys Rev Lett* 113(4):045901.
14. Keys AS, Garrahan GP, Chandler D (2013) Calorimetric glass transition explained by hierarchical dynamic facilitation. *Proc Natl Acad Sci USA* 110(12):4482–4487.
15. Wang LM, Velikov V, Angell CA (2002) Direct determination of kinetic fragility indices of glassforming liquids by differential scanning calorimetry: Kinetic versus thermodynamic fragilities. *J Phys Chem* 117(15):10184.
16. DeBolt MA, Eastal AJ, Macedo PB, Moynihan CT (1976) Analysis of structural relaxation in glass using rate heating data. *J Am Ceram Soc* 59(1–2):16–21.
17. Mari R, Kurchan J (2011) Dynamical transition of glasses: From exact to approximate. *J Chem Phys* 135(12):124504.
18. Krzakala F, Zdeborová L (2009) Hiding quiet solutions in random constraint satisfaction problems. *Phys Rev Lett* 102(23):238701.
19. Kraichnan R (1962) Stochastic models for many body systems. II. Finite systems and statistical nonequilibrium. *J Math Phys* 3(3):496.
20. Kurchan J, Parisi G, Zamponi F (2012) Exact theory of dense amorphous hard spheres in high dimension I. The free energy. *J Stat Mech* 2012:P10012.
21. Hansen JP, McDonald IR (2006) *Theory of Simple Liquids* (Academic, New York).
22. Charbonneau B, Charbonneau P, Jin Y, Parisi G, Zamponi F (2013) Dimensional dependence of the Stokes-Einstein relation and its violation. *J Chem Phys* 139(16):164502.
23. Mezard M, Parisi G, Tarzia M, Zamponi F (2011) On the solution of a ‘solvable’ model of an ideal glass of hard spheres displaying a jamming transition. *J Stat Phys* 2011: P03002.
24. Monasson R (1995) Structural glass transition and the entropy of the metastable states. *Phys Rev Lett* 75(15):2847–2850.
25. Kurchan J, Parisi G, Urbani P, Zamponi F (2013) Exact theory of dense amorphous hard spheres in high dimension. II. The high density regime and the Gardner transition. *J Phys Chem B* 117(42):12979–12994.
26. Charbonneau P, Kurchan J, Parisi G, Urbani P, Zamponi F (2014) Fractal free energy landscapes in structural glasses. *Nat Commun* 5:3725.
27. Lopatin AV, Ioffe LB (2002) Structural glass on a lattice in the limit of infinite dimensions. *Phys Rev B* 66(17):174202.
28. Montanari A, Ricci-Tersenghi F (2004) Cooling-schedule dependence of the dynamics of mean-field glasses. *Phys Rev B* 70(13):134406.
29. Rainone C, Urbani P, Yoshino H, Zamponi F (2015) Following the evolution of hard sphere glasses in infinite dimensions under external perturbations: Compression and shear strain. *Phys Rev Lett* 114(1):015701.
30. Krzakala F, Zdeborová L (2013) Performance of simulated annealing in p-spin glasses. *J Phys Conf Ser* 473(1):012022.